# The mutual diffusion coefficient for the van der Waals binary mixtures of types II, III, IV, and V

R. Castillo, C. Garza, and H. Dominguez
*Instituto de Fisica, UNAM, P.O. Box 20-364, D.F.01000 Mexico*

In the framework of the mean-field kinetic variational theory, a numerical study is presented to understand the concentration dependence of the mutual diffusion coefficient in terms of molecular sizes and interaction parameters for the van der Waals binary mixtures of types II, III, IV, and V, in the scheme of Scott and van Konynenburg. This work is an extension to the study for systems of type I presented by us quite recently. In addition, the behavior of the mutual diffusion coefficient of the van der Waals mixture is compared with that of the hard-sphere mixture and for the case of systems of type II, with experimental data of actual systems: water/$n$-propanol, $n$-hexane/acetone, and $n$-heptane/acetone. The mutual diffusion coefficients for the last two systems were determined by us with the Taylor dispersion technique. The mutual diffusion coefficients for the systems $n$-hexane/acetone and $n$-heptane/acetone are reported here at 298.15 and 303.15 K, respectively, along all the concentration range. The explicit model used here allows us to obtain an explanation about the role played by the variables that determine the concentration dependence of the mutual diffusion coefficient for actual systems.

## I. INTRODUCTION

There are very few model mixtures for which theory can be handled, almost without approximations, to give explicit equations relating the molecular parameters to the mutual diffusion coefficient (MDC). One of these is the van der Waals binary mixture. In a previous paper[1] (hereafter referred to as I), we obtained explicit expressions for the MDC for the van der Waals mixture in terms of molecular parameters in the framework of the mean-field kinetic variational theory. Our final formula was the same as that given by Karkheck et al.,[2] but our procedure had an additional practical advantage. The explicit dependence of the tail contribution was handled in such a way that the structure of the equations was the same as that given in the revised Enskog theory (RET) for hard-sphere systems.[3] This made easier the task of developing numerical solutions to calculate the MDC. In particular, comparisons between the mean-field kinetic variational theory and the RET are very simple within our framework, since we only need to turn off the tail contribution to recover the MDC as given in the RET. Moreover, in I, the MDC was related to the classification scheme devised by Scott and van Konynenburg[4] to study fluid phase equilibria in binary systems in a systematic way, and the global behavior of the MDC for systems of type I was studied. The link between the MDC and fluid phase equilibria can be traced to the fact that the behavior of the MDC is equal to that of the free energy curvature of the binary mixture, modulated by a compressibility factor, and other factors related to the dynamics of the two-particle collision.[1,2] On the other hand, the free energy curvature in a binary mixture is also responsible for the specific characteristics of the equilibrium phase diagrams.[4]

In this paper, a numerical study is presented to understand the effect of molecular sizes and interaction parameters on the concentration dependence of the MDC for the van der Waals binary mixtures of types II, III, IV, and V in the scheme of Scott and van Konynenburg. Moreover, we shall show that this procedure can be very useful to predict the most important features of the MDC versus concentration curves for actual systems. This paper is a natural extension of our work for mixtures of type I,[1] that allows us to obtain a complete picture of the way in which the interaction parameters modify the behavior of MDC in the van der Waals mixture. In particular, the parameter $\Lambda$ (difference in attractive forces between like and unlike pair of molecules), and the parameter $\xi$ (size difference between unlike pair of molecules) are the parameters that mainly determine the global behavior of the MDC.

Another important theory developed to understand transport properties in liquid mixtures is the RET, since it is a kinetic theory for hard-sphere fluids beyond the low density limit, that can give explicit calculations.[3,5] The first computer simulation studies to test the predictions for the MDCs given in the RET have been presented quite recently by Erpenbeck.[6-8] This author has studied equimolar mixtures having a diameter ratio of 0.4, a mass ratio of 0.03, at volumes in the range 20 to 1.7 times the close-packed volume. He found that the MDC drops monotonically to roughly 0.75 of the RET values when the density is increased. Notwithstanding those studies, it is still an open question to what extent the RET can correctly predict the MDC for binary mixtures of hard spheres. More simulation studies are needed to understand the contribution of correlated motion to the MDC in hard-sphere mixtures.

Simulations in binary liquid systems with a somewhat realistic intermolecular model potential are scarce. The best model potential studied has been the Lennard-Jones potential.[9-14] The works here were first devoted to developing accurate techniques,[9-11] then to studying the role of cross correlation in equimolar mixtures,[12] and in the last works[13,14] to studying how the particle volumes and the interaction strengths affect the MDC for equimolar mixtures. The results indicate that the MDC is very sensitive to the particle vol-

umes and to the interactions strengths, particularly to the cross parameters, but from those simulations it is difficult to obtain a clear picture of the role played by the molecular parameters.

An outline of the paper is as follows. In Sec. II, we review the most relevant points of the theory presented in our earlier paper[1] on which the present work is based. Section III is devoted to presenting a numerical study to understand how the different parameters involved in the van der Waals theory affect the concentration dependence of the MDC for systems of type II, III, IV, and V. For determining the usefulness of our approach to predict MDC of actual systems, experimental data for binary systems are needed. In this paper, we shall restrict our study to make comparisons for actual systems of type II only. The experimental data were obtained from the literature and from direct experimental determinations using the Taylor dispersion technique. In Sec. IV, we present the experimental procedure used to obtain the MDCs for the systems $n$-hexane/acetone and $n$-heptane/acetone. In Sec. V, calculations are presented for three actual systems belonging to the phase diagrams of type II, along all the concentration range: $n$-hexane/acetone, $n$-heptane/acetone, and water/$n$-propanol. These calculations are compared with experimental data and with calculations performed with the RET.

## II. THEORY

### A. Kinetic theory

Relevant among the kinetic equation approaches to liquid state are the mean-field kinetic variational theories.[15–18] Their development is an extension to include the case of particles interacting through a pair potential consisting of a hard-sphere core and an arbitrary soft attractive tail. One kinetic equation of this family, where the Kac limit can be successfully done, has been derived by Karkheck et al.[2] maximizing the entropy with certain simple constraints. We call this theory KVT I.[1,16] In this theory, the ratio of the generic two-particle distribution function to the product of the two one-particle functions is the pair distribution function, $g_2^{HS}(\mathbf{r}_1,\mathbf{r}_2|n)$, of a hard-sphere system in inhomogeneous equilibrium.[2,15] The result is a kinetic equation that embodies the exact thermodynamic description of a system interacting with a potential consisting of a hard-sphere core and an infinitely weak long-range attraction, i.e., the van der Waals interaction.[19]

The kinetic mean-field theory with the abovementioned limit can yield an expression for the MDC that exhibits a dependence on the tail strength. The expression for the MDC within this formalism is given in such a way that it can be related to the curvature of the free energy of the binary mixture.[1,2] The free energy curvature in a binary mixture is also responsible for the specific characteristics of the equilibrium phase diagrams. Those characteristics for this model mixture have been classified in a scheme devised by Scott and van Konynenburg.[4] This scheme allowed these authors to reproduce most of the known types of fluid–fluid phase equilibria observed in actual binary fluid mixtures. The relation between the free energy curvature and the MDC has

yielded a useful way to describe the global behavior of MDC on the same basis as the phase diagrams.[1,20] This was the case for the systems of type I studied in I. We shall show below that this procedure is also useful for studying the MDC of the remaining phase diagram types in the Scott and van Konynenburg convention.

The specific details to obtain explicit expressions for the MDC were presented in terms of molecular parameters in I. Our final formula was the same as that given by Karkheck et al.,[2] but our procedure had the practical advantage of giving the tail contribution in such a way that the structure of the equations was the same as that for the case of hard spheres. Therefore, the task of developing numerical solutions for calculating the MDC of van der Waals mixtures followed the same line of reasoning as the method presented by Lopez de Haro et al.[3] for the RET. The results were excellent. Here, we shall follow the same procedure used in I to study the systems of type II, III, IV, and V.

The macroscopic isothermal isobaric mass diffusion coefficient $D_{ij}^{c.m.}$ for a binary system is explicitly defined by the relation

$$\mathbf{J}_i = -\sum_{j=1}^{2} (1 - \delta_{jL}) D_{ij}^{c.m.} m_j \frac{\partial}{\partial \mathbf{r}} n_j, \tag{1}$$

where the $\mathbf{J}_i^{(1)}$ are the macroscopic mass fluxes to the first order in the gradients, relative to the local center-of-mass velocity. The present paper will follow the notation given in I.

In binary mixtures there is only one independent diffusion coefficient.[21] Equation (1) has been written in such a way that all the gradients occurring there are independent. The expression for the MDC for the van der Waals binary mixture in the KVT I, as shown in I, can be written as

$$D_{11}^{c.m.} = (\rho_1/2m_1 n^2) \sum_{j=1}^{2} d_{1,0}^{(j)} [E_{j1} - (P_1/P_L) E_{jL}], \tag{2}$$

where

$$P_i = \sum_{j=1}^{2} E_{ji}, \quad E_{ij} = (n_i/k_B T) \left( \frac{\partial \mu_i}{\partial n_j} \right)_{T, n_{k \neq j}}, \tag{3}$$

and the $d_{1,0}^{(k)}$ are the coefficients that appear in the Sonine polynomial expansion. For details see I. In order to obtain practical results, one restricts the number of Sonine polynomials in the expansion. We adopted here, as in I, the convention usually called the $N$th Enskog approximation, i.e., only $N$ Sonine polynomials are taken into account. The dependence on the tail contribution in Eq. (2) comes through the chemical potential. The coefficients $d_{1,0}^{(i)}$ depend on the hard core part of the interaction only. Expression (2) is useful to make comparisons between the KVT I and the RET, since we only need to turn off the tail contribution to recover the MDC given in the RET.

Equation (2) can be used for calculating the MDC in binary mixtures, but if one is interested in comparisons with experimental MDCs of actual mixtures, some additional calculations are needed. From the experimental point of view, the natural MDCs are those given relative to the mean vol-

ume velocity. Therefore, a transformation is needed. The relationship between the MDC for a binary mixture relative to the local center-of-mass velocity $D_{11}^{c.m.}$ and to the mean volume velocity $D_{11}^{v}$ is given by[1,21]

$$D_{11}^{v} = (\rho \bar{\nu}_2) D_{11}^{c.m.}, \tag{4}$$

where $\bar{\nu}_2$ is the partial specific volume of component 2. For details see Ref. 1.

## B. The Scott and van Konynenburg scheme

The classification scheme devised some time ago by Scott and van Konynenburg[4] used the van der Waals equation of state in a systematic study of fluid phase equilibria. They characterized the mixtures by three adimensional parameters:

$$\xi = (b_{22} - b_{11})/(b_{11} + b_{22}), \tag{5a}$$

$$\zeta = \left( \frac{a_{22}}{b_{22}^2} - \frac{a_{11}}{b_{11}^2} \right) \Big/ \left( \frac{a_{11}}{b_{11}^2} + \frac{a_{22}}{b_{22}^2} \right), \tag{5b}$$

$$\Lambda = \left( \frac{a_{11}}{b_{11}^2} - \frac{2a_{12}}{b_{11}b_{22}} + \frac{a_{22}}{b_{22}^2} \right) \Big/ \left( \frac{a_{11}}{b_{11}^2} + \frac{a_{22}}{b_{22}^2} \right). \tag{5c}$$

For $\xi = 0$, $\zeta$ is related to the difference in critical temperatures or pressures of the pure components, and $\Lambda$ is related to the molar heat of mixing. The van der Waals constants $a_m$ and $b_m$ for the mixture depend upon mole fraction $x_i$ as

$$a_m = \sum_{ij}^{2} x_i x_j a_{ij}, \quad b_m = \sum_{ij}^{2} x_i x_j b_{ij}. \tag{6}$$

The constants $a_{11}$ and $a_{22}$ measure the attractive forces between pairs of molecules of the pure components 1 and 2, respectively, and $a_{12}$ is the corresponding parameter for the interaction between molecules 1 and 2. The constants $b_{11}$, $b_{22}$, and $b_{12}$ are the size parameters for the pure components and for mixed pairs, respectively. Here, in agreement with the Scott and van Konynenburg convention,[4] we have used for the cross interaction

$$b_{12} = (b_{11} + b_{22})/2. \tag{7}$$

Scott and Van Konynenburg[4] distinguished in the $(\Lambda, \zeta)$ space five different regions, where fluid phase equilibria diagrams can be grouped according to the configuration of the critical lines and the three-phase lines on the $P-T$ diagram. They recognized a sixth type of diagram, but it was not among those predicted by the van der Waals equation. For details see Ref. 19 or Fig. 1 presented in I.

## III. MUTUAL DIFFUSION COEFFICIENTS FOR SYSTEMS OF TYPE II–V

For several van der Waals liquid binary mixtures, the MDCs were calculated through Eqs. (2) and (4) in the third Sonine approximation. They were denoted by $D_{11}$; the index $v$ will be used when it is necessary only. The parameters of the liquid mixtures were selected to fall into the diagrams of the type II, III, IV, and V of the Scott–van Konynenburg classification scheme. In this section, we shall present a numerical study to understand the influence of each parameter

on the MDC. Moreover, several calculations for hard-sphere mixtures are presented to show the difference between the RET and the KVT I predictions.

There are several sets of parameters that can be used to define a binary mixture under study. We have used the following set: $m_1$, $m_2$, $a_{22}$, $b_{22}$, $\Lambda$, $\xi$, $\zeta$, $n$, $T$, and $X_2$. Once this set is given, the other interaction parameters can be obtained with the following equations:

$$b_{11} = \frac{[1 - \xi] b_{22}}{[1 + \zeta]}, \tag{8}$$

$$a_{11} = \frac{[1 - \zeta]}{[1 + \zeta]} \cdot \frac{[1 - \xi]}{[1 + \xi]^2} b_{22}, \tag{9}$$

$$a_{12} = \frac{[1 - \xi]}{[1 + \xi]} \cdot \frac{[1 - \Lambda]}{[1 + \zeta]} a_{22}. \tag{10}$$

To make the interpretation of the obtained results in this numerical study easier, some of the abovementioned parameters are fixed for all the calculations. As a final goal, we shall use the procedure presented here to understand the behavior of the concentration dependence of the MDC for actual binary mixtures. Therefore, we selected the fixed parameters close to that of simple fluids, like liquid argon. These fixed parameters are $m_1 = m_2 = 6.6335 \times 10^{-23}$ g, $a_{22} = -1.305$ L$^2$ at mol$^{-2}$, $b_{22} = 49.79 \times 10^{-3}$ L mol$^{-1}$, $T = 168$ K, and $n = 2.03 \times 10^{22}$ L$^{-1}$.

Several tests showed that the calculated coefficients with respect to the mean volume velocity have the property[22] $D_{11}^{v} = D_{22}^{v}$. The selection of the most convenient Enskog approximation to be used in this procedure was discussed in I. The calculations reported here will be in the third Enskog approximation.

The effect of the parameter $\Lambda$ on the MDC is presented in Figs. 1 and 2. Here, all the calculations were done at $\xi = 0$. The results presented in these figures are quite reasonable, since $\Lambda$ measures the preference of the molecules of the system to interact with unlike molecules and to blend them. Therefore, for systems of the type II, III, and IV ($\Lambda > 0$, Fig. 1) we observe a decrease in the capacity of diffusion. The larger the $\Lambda$ the lesser diffusion. On the contrary, for systems of type V ($\Lambda < 0$, Fig. 2) the MDC increases as the $\Lambda$ decreases. This last result is the same as that found for systems of type I, also with $\Lambda < 0$, presented in our previous paper I. For comparison, in Figs. 1 and 2, we have included calculations for hard-sphere mixtures obtained by turning off the interaction tails. As is clearly presented in Figs. 1 and 2, hard-sphere theory cannot give any of the features obtained with the van der Waals model.

The effect of changing the tail interaction between particles of the same species in the fluid mixture modifies the $D_{11} - X_2$ diagrams in an important way. As an example of this effect, we present Figs. 3 and 4. In these figures several calculations for van der Waals binary mixtures corresponding to the diagrams of types II, III, IV, and V are presented, where the value of $a_{22}$ has been varied. All these calculations were done at $\xi = 0$. As the interaction between like-molecules is increased ($a_{22}$ more negative) systems of types II [Fig. 3(a)], III [Fig. 3(b)], and IV [Fig. 4(a)] lose their capability
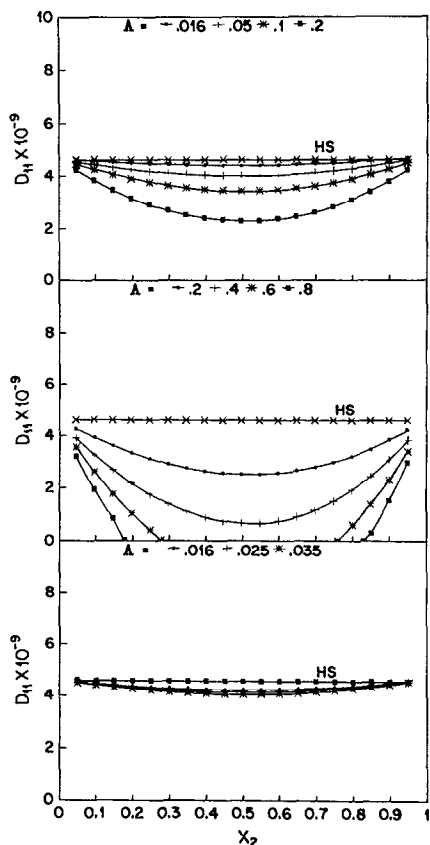
FIG. 1. The effect of the parameter $\Lambda$ on the mutual diffusion coefficient for the van der Waals mixtures II, III, and IV ($\Lambda > 0$). (a) Upper panel: type II ($\zeta = 0.3$ and $\xi = 0$); (b) middle panel: type III ($\zeta = 0.58$ and $\xi = 0$); (c) lower panel: type IV ($\zeta = 0.58$ and $\xi = 0$). HS denotes calculations for hard-sphere mixtures (RET).



FIG. 3. The mutual diffusion coefficient for van der Waals binary mixtures of types II and III ($\Lambda > 0$), where the value of $a_{22}$ has been varied. (a) Upper panel: type II ($\Lambda = 0.1$, $\zeta = 0.3$, and $\xi = 0$); (b) lower panel: type III ($\Lambda = 0.4$, $\zeta = 0.58$, and $\xi = 0$). HS denotes calculations for hard-sphere mixtures (RET).

demixed ($\Lambda > 0$) no matter what the value of $a_{22}$. Therefore, systems of types II, III, and IV have a tendency to lower their capacity to diffuse. On the contrary, systems of type V increase their capacity to diffuse. However, in addition to the conditions imposed by the value of $\Lambda$, as the interaction between molecules of compound 2 is increased, the system

to diffuse. For systems of type V [Fig. 4(b)] we found the opposite. Qualitatively, our interpretation is as follows: Since $\Lambda$ measures the preference of the molecules of the system to interact with unlike molecules, the molecules in the mixture will prefer depending on the sign of $\Lambda$, to be mixed ($\Lambda < 0$) or
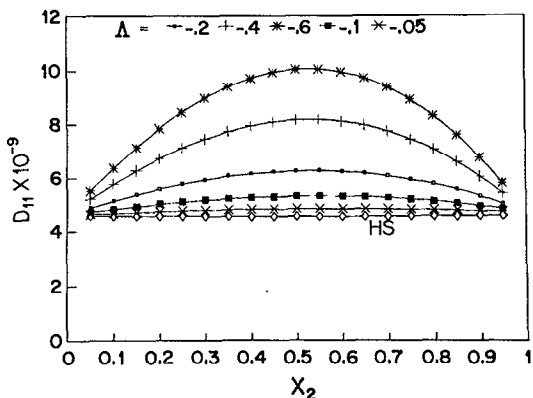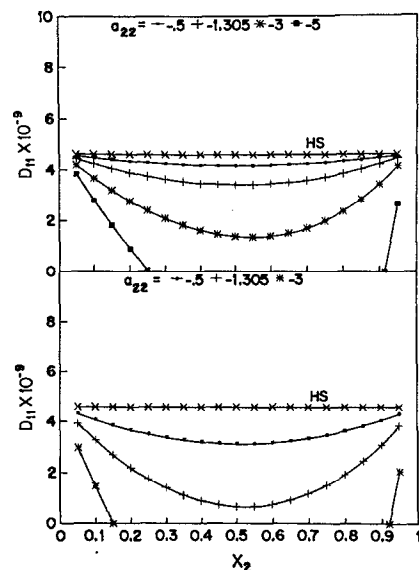


FIG. 2. The effect of the parameter $\Lambda$ on the mutual diffusion coefficient for the van der Waals mixtures V ($\Lambda < 0$). Type V ($\zeta = 0.58$ and $\xi = 0$). HS denotes calculations for hard-sphere mixtures (RET).
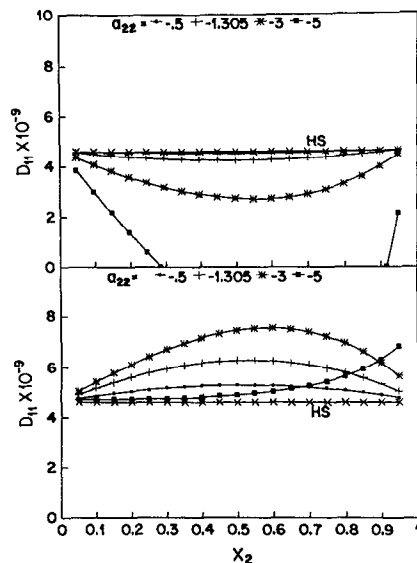


FIG. 4. The mutual diffusion coefficient for van der Waals binary mixtures of types IV ($\Lambda > 0$) and V ($\Lambda < 0$), where the value of $a_{22}$ has been varied. (a) Upper panel: type IV ($\Lambda = 0.016$, $\zeta = 0.58$, and $\xi = 0$); (b) lower panel: type V ($\Lambda = -0.2$, $\zeta = 0.58$, and $\xi = 0$). HS denotes calculations for hard-sphere mixtures (RET).
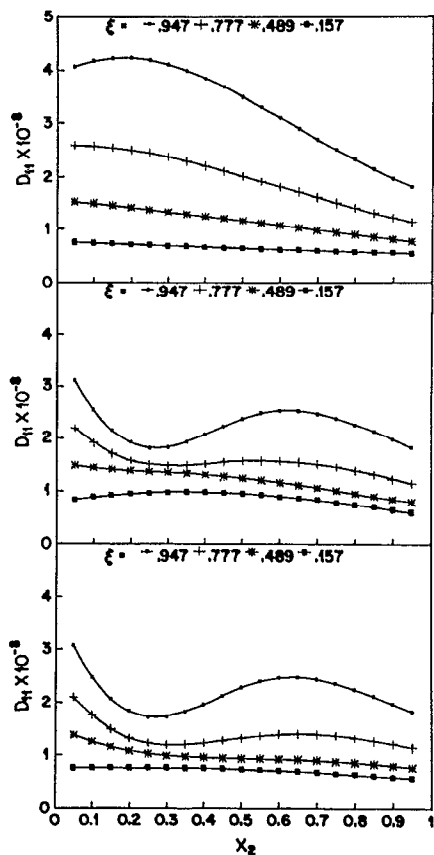
FIG. 5. The effect of the molecular volume on the $D_{11}-X_2$ diagrams. (a) Upper panel: hard-sphere mixture (RET); (b) middle panel: van der Waals mixture of type I ($\Lambda=-0.2$ and $\zeta=0$); (c) lower panel: van der Waals mixture of type II ($\Lambda=0.1$ and $\zeta=0.3$).
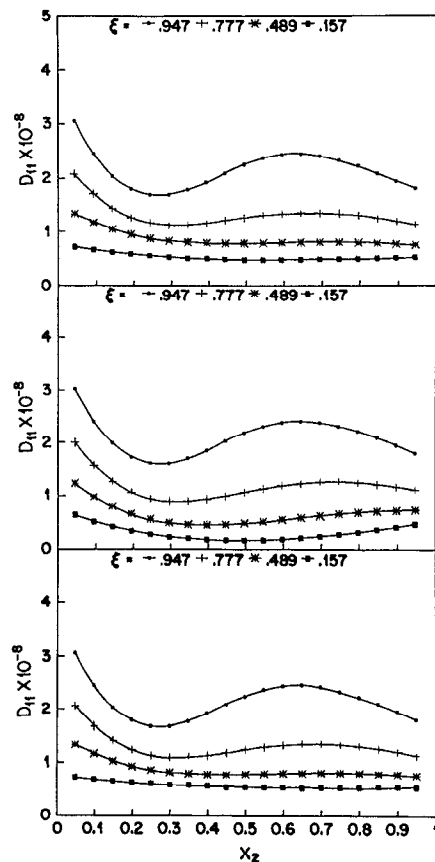
FIG. 6. The effect of the molecular volume on the $D_{11}-X_2$ diagrams. (a) Upper panel: van der Waals mixture of type III ($\Lambda=0.4$, $\zeta=0.58$); (b) middle panel: van der Waals mixture of type IV ($\Lambda=0.016$ and $\zeta=0.58$); (c) lower panel: van der Waals mixture of type V ($\Lambda=-0.2$ and $\zeta=0.58$).

responds to the concentration fluctuations in promoting diffusion in the sense that the molecules of compound 2 can be, as far as possible, close together. Therefore, in systems of types II, III, and IV, the MDC falls down as the $a_{22}$ interaction is increased. For the particular parameters used in the calculations for the systems of types II, III, and IV, the systems of type III are the most affected. Since they have the lower cross interaction $a_{12}$, as can be seen from Eq. (10). The minima of the $D_{11}-X_2$ curves shown in Figs. 3 and 4(a) move toward the region rich in compound 2, since the interaction between molecules of compound 2 is a little bit stronger than between molecules of compound 1. For the systems of type V [Fig. 4(b)] the interpretation is more involved. Here the value of $\Lambda$ asks the system for increasing the diffusion; on the other hand, the increasing values of $a_{22}$ push in the opposite direction. In this particular example, at low values of $a_{22}$, all seems to indicate that the cross interaction $a_{12}$ wins over the like-molecules interactions $a_{ii}$. But at some extreme values of $a_{22}$ the diffusion begins to decrease. Figure 4(b) shows this contest between interactions. For values $a_{22}$ a little bit below $-3$, the $D_{11}-X_2$ diagrams start their drop. In Fig. 4(b), only the calculations for $a_{22}=-5$ are presented. In this case, the MDC grows with the mole fraction of compound 2 in a way suggesting that the system facilitates the departure of molecules of species 1, during the

concentration fluctuations, making it possible to leave the system richer in compound 2.

The effect of molecular volume will be discussed now. The effect of changing the molecular volume in the van der Waals mixtures of types II, III, IV, and V can be obtained from Figs. 5 and 6. In Figs. 5 and 6, the MDCs for several binary systems as a function of the concentration are presented for four values of $\xi$ (0.157, 0.489, 0.777, and 0.947). In all these calculations the number density is constant. In Figs. 5(a) and 5(b), calculations for hard-sphere mixtures and for van der Waals mixtures of type I ($\Lambda=-0.2$, $\zeta=0$) were included to make comparisons. This will help us to give a complete picture of the effect of the molecular volume on the MDC. Thus, in Fig. 5(a) calculations without tail interactions are presented. Our interpretation for this case follows from our earlier discussion in I: At low $\xi$, the MDC decreases as the concentration of the larger component (2) goes to 1. Since the number density was a constant the mixture has less molecules of component 1, thus the larger molecules do not have enough room to diffuse. Therefore, the larger molecules block their motion themselves; like a cage effect. At greater values of $\xi$, the $D_{11}-X_2$ diagrams suggest[1] that the diffusion process increases due to the motion of small molecules through the free space left by the larger molecules, and at
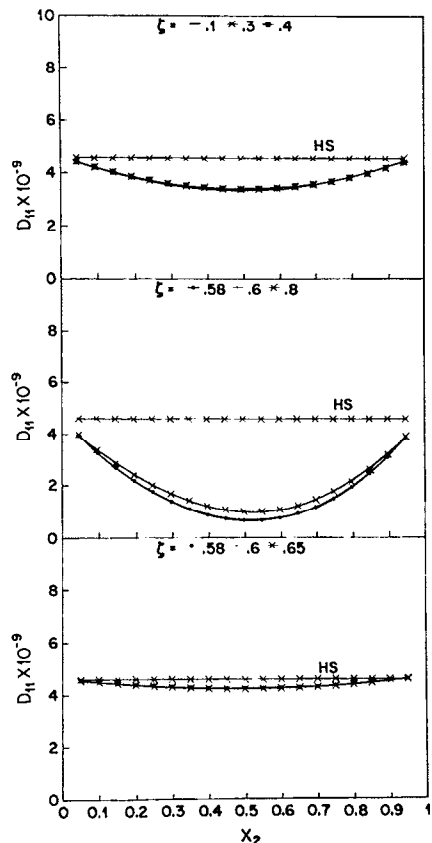
FIG. 7. The effect of the parameter $\zeta$ on the concentration dependence of the MDC for systems of types II, III, and IV ($\Lambda > 0$). (a) Upper panel: type II ($\Lambda = 0.1$ and $\xi = 0$); (b) middle panel: type III ($\Lambda = 0.4$ and $\xi = 0$); (c) lower panel: type IV ($\Lambda = 0.016$ and $\xi = 0$). HS denotes calculations for hard-sphere mixtures (RET).



FIG. 8. The effect of the parameter $\zeta$ on the concentration dependence of the MDC for systems of type V ($\Lambda = -0.2$ and $\xi = 0$). HS denotes calculations for hard-sphere mixtures (RET).

some large values of $\xi$ a maximum in the $D_{11} - X_2$ diagram is observed

In general, the MDC of the van der Waals mixtures increases with the parameter $\xi$, and the $D_{11} - X_2$ diagrams have the same concentration dependence pattern. This suggests that diffusion through the holes left by the larger molecules is as important as in the hard-sphere system [Fig. 5(a)]. Therefore, the situation for van der Waals mixtures is much more complicated, since we have two effects competing: the volume asymmetry and the attractive tail interactions. At low $\xi$, the effect of the interaction between different molecules, determined by the sign of $\Lambda$, is dominant. Therefore, the MDCs for the systems of types II, III, and IV ($\Lambda > 0$) are little below that of the hard-sphere system for the same values of $\xi$. Just the opposite occurs for systems of types I and V ($\Lambda < 0$), in agreement with the sign of $\Lambda$. At higher $\xi$, although the main trend of the $D_{11} - X_2$ curves of the hard-sphere system is inherited by the van der Waals systems, the interaction can completely change these curves. In our particular examples for the van der Waals systems shown in Figs. 5 and 6, a minimum in the $D_{11} - X_2$ is observed as the $\xi$ becomes larger. Our interpretation for these calculations is as follows: As we mentioned for the hard-sphere system, the diffusion process increases as the param-
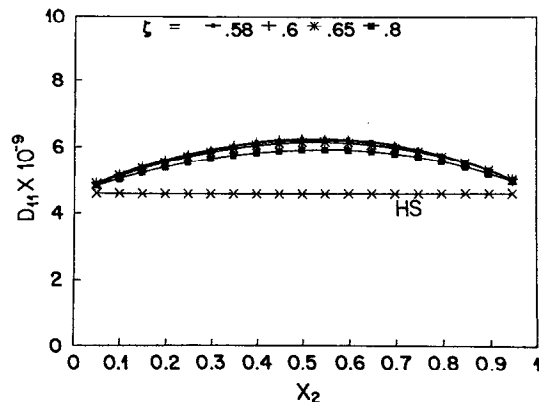
eter $\xi$ increases due to the motion of small molecules through the free space left by the larger molecules. For van der Waals mixtures this seems to be the same. But, when the attractive tails are turned on in these particular examples the interaction $a_{22}$ is more important than the interactions $a_{11}$ and $a_{12}$. See Eqs. (9) and (10). Therefore, the motion of the small molecules (1) through the free space left by the larger molecules (2) is reduced, since the large interaction between molecules of type 2 tends to make them closer, thus leaving less room for intermixing. As the concentration of molecules 2 is so large the larger molecules do not have enough room to diffuse, they block their motion themselves as in the hard-sphere system. Therefore, the MDCs at these concentrations are very close to that of the hard-sphere system.

Figures 7 and 8 show the dependence of the $D_{11} - X_2$ diagrams on the parameter $\zeta$ for van der Waals mixtures of types II, III, IV, and V. Here, the main trend follows from $\Lambda$. Systems of types II, III, and IV ($\Lambda > 0$, Fig. 7) present a lower diffusion than the hard-sphere system obtained by turning off the attractive tail potential. Here, it is clearly shown that the larger the parameter $\Lambda$ the lower the MDC. For systems with $\Lambda < 0$, i.e., systems of type V, the diffusion process is increased with respect to the hard-sphere system. This behavior agrees with the fact that $\Lambda$ measures the preference of the molecules of the system to interact with unlike molecules and to blend them. Within this major trend, the variation of parameter $\zeta$ that measures the relative strength of the interaction between particles 2 with respect to particles 1 is not very important. As expected, for systems of type V presented in Fig. 8, our calculations suggest that as the interaction between particles 2 begins to grow the diffusion process begins to decline, in spite of the negative value of $\Lambda$.

## IV. EXPERIMENT

In this section, the experimental details to obtain the MDCs in the systems acetone/$n$-hexane and acetone/$n$-heptane along all the concentration range are presented. These data will be used to test the predictions of the van der Waals model in Sec. V.

TABLE I. Mutual diffusion for the system $n$-hexane/acetone at 298.15 K.

| Acetone mole fraction | $D_{11}^v \times 10^9$ (m$^2$ s$^{-1}$) |
| --- | --- |
| 0.9997 | 4.28 |
| 0.7419 | 2.17 |
| 0.5016 | 1.81 |
| 0.2479 | 2.25 |
| $3.7533 \times 10^{-4}$ | 3.10 |

TABLE II. Mutual diffusion for the system $n$-heptane/acetone at 303.15 K.

| Acetone mole fraction | $D_{11}^v \times 10^9$ (m$^2$ s$^{-1}$) |
| --- | --- |
| 0.9986 | 4.23 |
| 0.7541 | 1.75 |
| 0.4936 | 1.87 |
| 0.2477 | 2.28 |
| $2.3673 \times 10^{-4}$ | 4.25 |

## A. Instrument design and operation

The Taylor dispersion is based on the dispersion of an injected binary mixture pulse in a laminar flowing stream of the same mixture at slightly different composition, by the joint action of convection and molecular diffusion. Under proper conditions, the pulse concentration profile will eventually become normal, and the center of gravity of the profile will move with the mean velocity of laminar flow. The theory for the development of an ideal equipment to measure MDCs with this method is reviewed by Alizadeh et al.[23] Furthermore, they presented detailed criteria for the design of a practical instrument. The details of our instrument were presented in Ref. 24.

Alizadeh et al.[23] derived expressions for the first ($\bar{t}$) and second ($\sigma^2$) temporal moments of the distribution of the dispersed pulse for an ideal instrument, and a set of corrections to this ideal instrument in order to include practical limitations. They found that the ideal moments have to be corrected according to

$$\bar{t} = \bar{t}_{\text{exp}} + \Sigma \, \delta \bar{t}_i \quad \text{and} \quad \sigma^2 = \sigma^2_{\text{exp}} + \Sigma \, \delta \sigma_i^2, \qquad (11)$$

where $\bar{t}_{\text{exp}}$ and $\sigma^2_{\text{exp}}$ denote the experimentally determined moments, and $\delta \bar{t}_i$ and $\delta \sigma_i^2$ are corrections to be applied to them. For details see Refs. 23 and 24.

The values of $\bar{t}_{\text{exp}}$ and $\sigma^2_{\text{exp}}$ were determined with a nonlinear fitting program of the digitized values corresponding to the analog signal of a differential refractometer, in the region where it has a linear response to the concentration difference between the cells. The acquisition of data were performed with a data acquisition board (PC-Lab Card 812PG, Advantech, Co. Ltd.), and a Printaform PC.

## B. Materials and precision

Heptane, hexane, and acetone of 99% purity were supplied by J. T. Baker Co. and Aldrich. Analyses by gas chromatography gave a value better than 99.9% purity. The binary mixtures were prepared with an estimated error in the quoted mole fractions to be less than $1 \times 10^{-4}$. Special care was taken to degas the binary mixtures in an ultrasonic cleaner, without inducing concentration changes, to prevent bubble formation during the experiment.

Measurements of MDCs were carried out in mixtures of $n$-hexane/acetone and $n$-heptane/acetone, along the range of concentration, at 298.15 and 303.15 K, respectively. The results are shown in Tables I and II. It is difficult to estimate the precision involved in the determination of MDCs by the technique described above. Hence, we followed the common practice of employing the reproducibility of the results of a

series of experiments, under nominally identical experimental conditions. We determined the values of $\bar{t}_{\text{exp}}$ and $\sigma^2_{\text{exp}}$ as mentioned above, and after doing the corrections discussed in Refs. 23 and 24, we obtained a precision of 2.5%.

## V. CALCULATIONS FOR ACTUAL MIXTURES OF THE TYPE II

For determining the usefulness of our procedure to predict MDCs for actual mixtures of type II, several coefficients $D_{11}^v$ were calculated and compared with experimental data for three binary systems along all the concentration range. This test is possible, if experimental MDCs are provided for mixtures previously classified as belonging to the diagrams of type II, in the Scott and van Konynenburg convention. Here, the systems under study were the following: $n$-propanol/water, acetone/$n$-hexane, and acetone/$n$-heptane. The high pressure phase equilibria of these systems show a continuous gas–liquid critical line between the critical points of the pure components,[25,26] in addition to the presence of liquid–liquid inmiscibility at relatively low temperatures. Acetone/$n$-hexane has a consolute point at 234 K,[27] and acetone/$n$-heptane at 245.5 K;[27] $n$-propanol/water has an estimated consolute point at 250 K by extrapolation.[27] We performed the calculations for these systems with the interaction parameters presented in Table III. The results are shown in Fig. 9 for several mole fractions. The experimental data for acetone/$n$-hexane and acetone/$n$-heptane were obtained by us as mentioned in Sec. III. The experimental data for $n$-propanol/water were obtained from Ref. 28. Here, the authors also used the Taylor dispersion technique.

As expected, when predictions for actual fluids are performed, the most difficult problem is to obtain a reliable set of interaction parameters. Here, an initial set of parameters

TABLE III. Parameters for the actual mixtures.

| | $n$-Hexane(1)/acetone(2) | $n$-Heptane(1)/acetone(2) |
| --- | --- | --- |
| $a_{22}$ | 15.0 | 10.0 |
| $b_{22}$ | 130.0 | 135.0 |
| $\Lambda$ | 0.08 | 0.1 |
| $\zeta$ | 0.35 | 0.30 |
| $\xi$ | −0.44 | −0.45 |

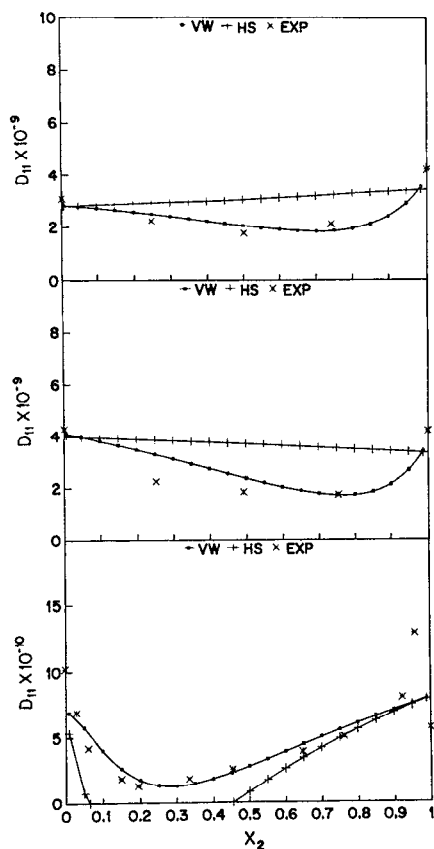| | Water(1)/propanol(2) |
| --- | --- |
| $a_{22}$ | 17.0 |
| $b_{22}$ | 245.0 |
| $\Lambda$ | 0.01 |
| $\zeta$ | −0.55 |
| $\xi$ | 0.70 |

FIG. 9. Comparison between experimental mutual diffusion coefficients (EXP), calculations using the van der Waals model (VW), and the hard-sphere theory (HS) for $n$-hexane/acetone (2) at 298.15 K (upper panel), $n$-heptane/acetone (2) at 303.15 K (middle panel), and water/$n$-propanol (2) at 298.15 K (lower panel).

was estimated as follows: Each component was modeled as a hard sphere of diameter $\sigma$ (Lennard-Jones length parameter), plus an attractive Lennard-Jones tail. The $a_{ii}$'s and $b_{ii}$'s can be estimated through standard formulas.[29] The Lennard-Jones parameters, $\sigma$ and $\epsilon$, were obtained from Ref. 30. The cross interactions were selected in such a way that the binary mixtures always fall into the region of the $\Lambda$-$\zeta$ diagram corresponding to the diagrams of type II (see Fig. 1 in I). Since our main interest was to understand how the different parameters affect the $D_{11} - X_2$ curves, we were not interested in developing a procedure to obtain the best parameters that match the experimental data. Moreover, it is not known to what extent the correlated motion affects the MDC. Therefore, any intent of quantitative fitting can be misleading. Thus, the initial set of interacting parameters was modified for each mixture, in such a way that one can obtain the form of the experimental $D_{12} - X_2$ curves. In this way, we arrived at the final set of interacting parameters given in Table III. One important point to mention is that the initial and the final sets of parameters are very close.

Figure 9 presents calculations for the systems $n$-propanol/water, acetone/$n$-hexane, and acetone/$n$-heptane along all the concentration range. In these three examples, we clearly see how the van der Waals model qualitatively

predicts the same concentration behavior as does the experimental data. The only feature that our model cannot properly describe is a thin peak reported in the $n$-propanol/water system close to $X_2=1$. We cannot explain this. But this reason is probably related to the fact that the van der Waals mixture is still too rough to deal with actual mixtures.

The different capability of the van der Waals model and of the hard-sphere model to predict the MDCs of actual mixtures can be compared. In Fig. 9, calculations for the MDCs given in the RET were also included in the third Enskog approximation. The hard-sphere diameters were exactly the same as those used for the van der Waals calculations, and Eq. (7) was used to define the volume cross interaction. The actual difference between the van der Waals and the RET calculations is the tail interaction. In general, the hard-sphere calculations cannot give the proper curvature shown by the experimental $D_{11} - X_2$ curves.

In summary, here and in our previous paper I, we have presented a complete scheme to understand the behavior of the MDC. In our model, the MDCs of liquid mixtures can be explicitly calculated. Moreover, we can understand how the different parameters affect the $D_{11} - X_2$ diagrams. On the other hand, the procedure we have followed can be used to correlate experimental data of actual mixtures, which requires very little input while still yielding reasonable qualitative good results. As we have shown, systems of types I[1] and II can be described by our method. Future work must be addressed to determine the usefulness of our procedure to explain the MDC for systems of types III, IV, and V, and to implement this scheme for barodiffusion and thermal diffusion. This work is underway and will be published shortly.

## ACKNOWLEDGMENTS

[1] R. Castillo, C. Garza, and H. Dominguez, J. Chem. Phys. **99**, 9899 (1993).
[2] J. Karkheck, E. Martina, and G. Stell, Phys. Rev. A **25**, 3328 (1982).
[3] M. Lopez de Haro, E. G. D. Cohen, and J. M. Kincaid, J. Chem. Phys. **78**, 2746 (1983).
[4] P. H. van Konynenburg and R. L. Scott, Philos. Trans. R. Soc. London **298**, 495 (1980); R. L. Scott and P. H. van Konynenburg, Discuss. Faraday Soc. **49**, 87 (1970).
[5] J. M. Kincaid, M. Lopez de Haro, and E. G. D. Cohen, J. Chem. Phys. **79**, 4509 (1983).
[6] J. J. Erpenbeck, Phys. Rev. A **39**, 4718 (1989).
[7] J. J. Erpenbeck, Phys. Rev. A **45**, 2298 (1992).
[8] J. J. Erpenbeck, Phys. Rev. E **48**, 223 (1993).
[9] D. L. Jolly and R. J. Bearman, Mol. Phys. **41**, 137 (1980).
[10] D. MacGowan and D. J. Evans, Phys. Rev. A **34**, 2133 (1986).
[11] M. Schoen and C. Hoheisel, Mol. Phys. **52**, 33 (1984).
[12] M. Schoen and C. Hoheisel, Mol. Phys. **52**, 1029 (1984).
[13] R. Vogelsang and C. Hoheisel, Phys. Rev. A **38**, 6296 (1988).
[14] J. M. Stoker and R. L. Rowley, J. Chem. Phys. **91**, 3670 (1989).
[15] J. Karkheck and G. Stell, J. Chem. Phys. **75**, 1475 (1981).
[16] G. Stell, J. Karkheck, and H. van Beijeren, J. Chem. Phys. **79**, 3166 (1983).
[17] W. Sung and J. S. Dahler, J. Chem. Phys. **80**, 3025 (1984).
[18] R. C. Castillo, E. Martina, M. Lopez de Haro, J. Karkheck, and G. Stell, Phys. Rev. A **39**, 3106 (1989).

[19] M. Kac, P. C. Hemmer, and G. E. Uhlenbeck, J. Math. Phys. **4**, 216 (1963).

[20] R. Castillo, M. E. Costas, and A. Robledo, Int. J. Thermophys. **10**, 427 (1989).

[21] S. R. De Groot and P. Mazur, *Nonequilibrium Thermodynamics* (Dover, New York, 1984).

[22] D. D. Fitts, *Nonequilibrium Thermodynamics* (McGraw-Hill, New York, 1962).

[23] A. Alizadeh, C. A. Nieto de Castro, and W. A. Wakeham, Int. J. Thermophys. **1**, 243 (1980).

[24] R. Castillo, H. Dominguez, and M. Costas, J. Phys. Chem. **94**, 8731 (1990).

[25] J. S. Rowlinson, and F. L. Swinton, *Liquids and Liquids Mixtures* (Butterworths, London, 1982).

[26] W. B. Kay, J. Phys Chem. (Ithaca) **68**, 827 (1964).

[27] A. W. Francis, *Critical Solution Temperatures*, Advances in Chemistry Series No. 31 (American Chemical Society, Washington, D. C., 1961).

[28] K. C. Pratt and W. A. Wakeham, Proc. R. Soc. London Ser. A **342**, 401 (1975).

[29] T. M. Reed and K. E. Gubbins, *Applied Statistical Mechanics* (McGraw-Hill, New York, 1973).

[30] C. Reid, J. M. Prausnitz, and T. K. Sherwood, *The Properties of Gases and Liquids*, 3rd ed. (McGraw-Hill, New York, 1979).